

AIAA 81-0335R

An Experimental Study of Hypersonic Cavity Flow

Donald E. Nestler*

General Electric Company, Philadelphia, Pa.

Nomenclature

A_B	= base area of model
C_N	= normal force coefficient; $C_N = F_N / q_\infty A_B$
F_N	= normal force
H	= window recess
L	= axial length of model (Fig. 1)
M	= Mach number
P	= static pressure
q	= dynamic pressure
R_N	= model nose radius
Re	= Reynolds number
X	= coordinate along window floor (Fig. 4)
X_M	= axial location measured from sharp apex
Y_M	= lateral location from window centerline (Fig. 3)
α	= angle of attack
δ	= boundary-layer thickness

Subscripts

W	= wall value
cone	= value on cone surface upstream of window
∞	= freestream value

Abstract

RECENT flight data suggest that antenna windows influence the trajectory deflections of a ballistic re-entry vehicle during movement of boundary-layer transition over the vehicle. The purpose of this study was to measure pressure distributions and force increments of idealized ablated windows (cavities) under hypersonic flow conditions. Results were found to be sensitive to the cavity aspect ratio and to the state of the upstream boundary layer.

Contents

An existing conical model (Fig. 1) was modified to incorporate a variety of simulated antenna window ablated shapes. Tests were conducted in AEDC Tunnel B at $M_\infty = 8$ over a range of Re_∞ of 1.0 to $3.3 \times 10^6/\text{ft}$. Seventy-five runs were made to determine the effect of window geometry, Reynolds number, nose bluntness, angle of attack, and window blowing rate on pressure distribution within and downstream of the window. Shadowgraphs and oil-flow photographs also were obtained to assist in interpreting the type of flow in the window cavity.

The model delivered to AEDC contained 70 pressure ports; of these, 32 ports were located in the basic cone frustum, while the remaining 38 were located in the window floor and surrounding insert. Figure 2 is a photograph of the pressure port locations in the window floor and backup piece. The staggered arrangement of ports on either side of the window centerline provided more detailed longitudinal pressure distribution, assuming negligible circumferential pressure

ALL DIMENSIONS IN INCHES

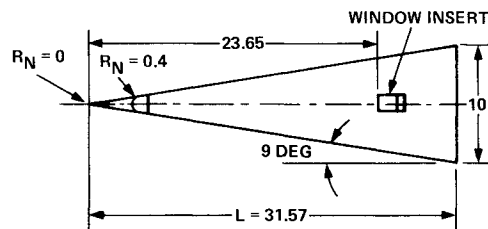


Fig. 1 Schematic of wind-tunnel test model.

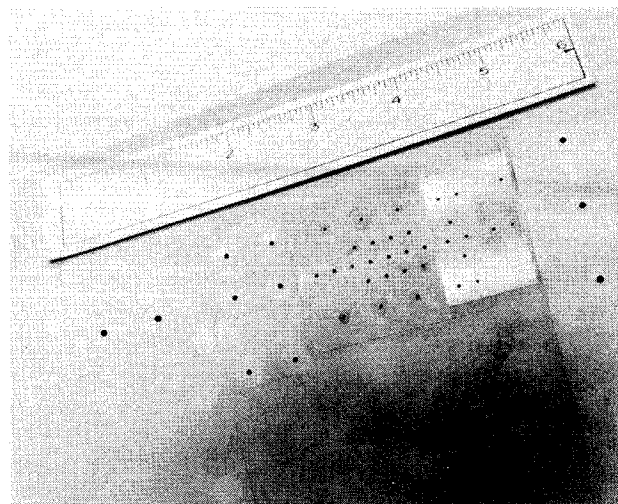


Fig. 2 Instrumented window.

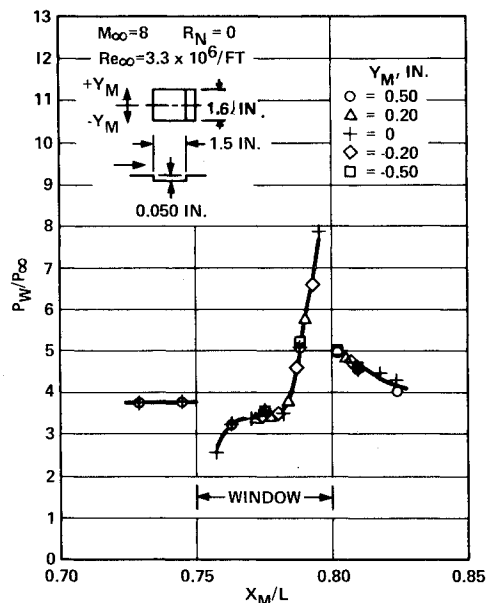


Fig. 3 Longitudinal pressure distribution (typical).

Presented as Paper 81-0335 at the AIAA 19th Aerospace Sciences Meeting, St. Louis, Mo., Jan. 12-15, 1980; submitted March 9, 1981; synoptic received Oct. 7, 1981. This paper is declared a work of the U.S. Government and therefore is in the public domain. Full paper available from AIAA Library, 555 W. 57th St., New York, N.Y. 10019; microfiche—\$3.00, hard copy—\$7.00. Remittance must accompany order.

*Staff Consultant. Member AIAA.

gradients. Incremental forces induced by the windows were determined by total model force measurements made with and without windows.

Figure 3 shows typical pressure data for the basic rectangular window at maximum Reynolds number and $R_N = 0$ (turbulent boundary layer, $\delta = 0.22$ in.). Note that an initial pressure decrease at the upstream end of the cavity is followed by a recovery to a level somewhat lower than the upstream pressure. A steep pressure rise then occurs in the downstream end of the window, followed by a decay back to cone pressure aft of the window. The lack of a pressure plateau upstream of the forward-facing step at the rear of the window is consistent with the data of Driftmyer,¹ at low values of H/δ . Integration of pressure plots such as those of Fig. 3 showed that the incremental normal force resulting from increased pressure aft of the window was comparable to the incremental normal force generated within the window.

Figure 3 also shows the lack of significant pressure variation in the circumferential direction. It can be inferred that the flow is essentially two-dimensional in a recessed window on an axisymmetric body at $\alpha = 0$. The window sidewalls probably act like fences to prevent the pressure rise resulting from the forward-facing step from causing significant three-dimensional flow effects. This result agrees with the data of Behrens,² who found that side fences produced a two-dimensional flow for a forward-facing step if the aspect ratio (transverse width/step height) was at least 19. In the present case, the window geometries with closed-cavity flow have aspect ratios from 16 to 32.

Figure 4 is a composite plot of mean lines drawn through various data sets such as that of Fig. 3. Two distinct types of pressure distribution are noted. For the shallower window recesses, the initial expansion at the upstream corner and the compression at the downstream corner become stronger as the window recess is increased from 0.050 in. However, the deeper window recesses (0.125 and 0.150 in.) exhibit only a mild reduction in pressure at the upstream corner, followed by a pressure rise in the downstream corner which is less than that of the shallow recesses. These pressure distributions are consistent with shadowgraphs which suggested a change in cavity flow structure for the deeper recesses (length-to-depth ratios of 12 or less). As such, these hypersonic results are consistent with the cavity flow criteria of Charwat³ for supersonic flow conditions.

Tests of the sharp nose model with Re_∞ reduced to $2.0 \times 10^6/\text{ft}$ or less produced a laminar boundary layer upstream of the cavity, with small pressure rise in and downstream of the cavity. Likewise, a blunt nose of $R_N = 0.4$ in. at maximum Re_∞ of $3.5 \times 10^6/\text{ft}$ also gave a laminar boundary layer, with small window pressure perturbations.

Axial and normal force increments due to the window were computed in two ways: 1) integration of pressure distributions and 2) force balance measurement. Comparison of the two methods showed a surprising degree of consistency, considering the difficulty in deriving accurate incremental forces from force-balance measurements on the entire model. This is illustrated by a plot of ΔC_N vs window recess (Fig. 5). The decrease in force as window recess increased above 0.100 in. is clearly delineated by either method. Figure 5 depicts the importance of understanding the fundamentals of cavity flow in order to model the forces associated with separated flow over recessed windows.

Incremental window forces developed in laminar flow were found to be negligible compared to window forces in transitional and turbulent flow; hence, an asymmetric transition

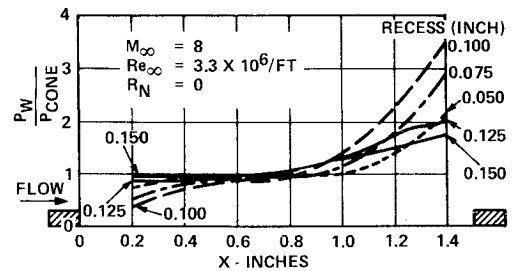


Fig. 4 Composite plot of window floor pressures - effect of recess.

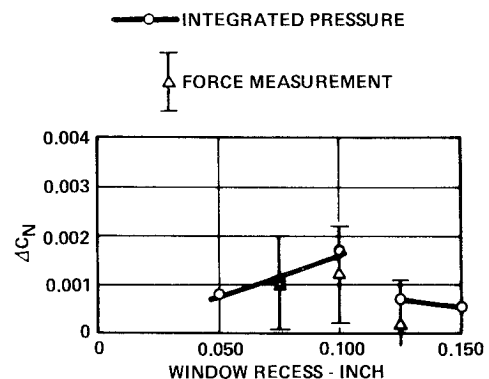


Fig. 5 Normal force increment vs window recess for $Re_\infty/\text{ft} = 3.3 \times 10^6$, $R_N = 0$.

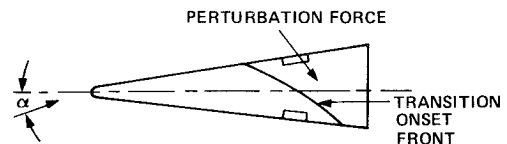


Fig. 6 Hypothesized trim induced by window/transition front interaction.

front will cause a window-induced trim, even if diametrically opposite windows have identical recesses (Fig. 6).

The wind-tunnel results presented herein extend separated-flow technology to include shallow cavities in hypersonic axisymmetric flow, with recesses much smaller than the boundary-layer thickness.

Acknowledgments

This work was performed as part of the Performance Technology Program-G II, under Air Force Contract F04701-78-C-0104. The support of A. Boudreau, D. Fikes, and J. Hahn of ARO in conducting the test program is acknowledged.

References

- Driftmyer, R.T., "A Forward Facing Step Study: The Step Height Less than the Boundary Layer Thickness," NOLTR 73-98, May 1973.
- Behrens, W., "Separation of a Supersonic Turbulent Boundary Layer by a Forward-Facing Step," AIAA Paper 71-127, Jan. 1971.
- Charwat, A.F., "Supersonic Flows with Embedded Shock Regions," *Advances in Heat Transfer*, Academic Press, New York, 1970.